arXiv:1111.4647v1 [quant-ph] 20 Nov 2011

Local description of the molecular Aharonov-Bohm effect

Jonas Larson,[1, 2, *] Elham Nour Ghassemi,[1, 3] and Åsa Larson[1]
[1]*Department of Physics, Stockholm University, SE-106 91 Stockholm, Sweden*
[2]*Institut für Theoretische Physik, Universität zu Köln, Köln, 50937, Germany*
[3]*Institut für Festkörpertheorie, Westefälische Wilhelms-Universität, Münster, 48149, Germany*

(Dated: November 22, 2011)

The Aharonov-Bohm effect is one of the most comprehensible examples of quantum non-locality. The so called molecular Aharonov-Bohm effect displays great similarities with the latter, but still, we show how this effect can be explained using arguments relying solely on locality, whereby we mean that the effect can be traced down to a force acting locally on the phase space distribution. Our method hinges on studying the system in its momentum representation, and introducing a "conjugate gauge potential" which render an everywhere non-zero synthetic magnetic field. The resulting Lorenz force induces a transverse current which can be attributed the equivalence of an intrinsic spin Hall effect. The idea is demonstrated for the linear $E\times\varepsilon$ Jahn-Teller model and applied to the Li$_3$ molecule, for which its corresponding Hamiltonian is obtained by diabatization of *ab intio* determined adiabatic potential energy surfaces.

PACS numbers: 31.50.Gh, 03.65.Vf

Introduction. – One of the most well known, and also most transparent, examples of quantum non-locality is the one by Aharonov and Bohm [1]; An electrically charged particle encircling a magnetic solenoid. Despite never being in direct contact with the magnetic field, the particle acquires a phase shift proportional to the magnetic flux through the loop traversed by the particle. The distance between the particle and the solenoid is not of importance, solely the fact that the particle's trajectory encircles the singular flux line. Non-locality, in general, results from the wave nature of the Schrödinger equation. In addition to the wave property, this equation is manifestly first order in time. Thus, all that is needed to achieve the complete system-evolution is the system's wave function at some time $t=0$, i.e. $\psi(\mathbf{x},0)$. Classically, on the other hand, a particle's trajectory depends both on its initial position $\mathbf{x}$ and its initial momentum $\mathbf{p}$. This distinctness of quantum mechanics has its origin in position and momentum being conjugate variables, e.g. knowing $\psi(\mathbf{x},t)$ gives you the corresponding momentum wave function $\phi(\mathbf{p},t)$ via a Fourier transform. Consequently, as the Heisenberg uncertainty relation also tells us, affecting one of the two variables will inevitably influence the other.

In this work we demonstrate how a situation seemingly non-local can be put in a local form by making explicit use of the inseparable connection between $\mathbf{x}$ and $\mathbf{p}$. The system we have in mind is of the Jahn-Teller (JT) type [2], more precisely the $E\times\varepsilon$ JT model. This has been a paradigm model in the chemical and the solid state physics communities for more than half a century [2, 3], and most recently it has also turned out to be of relevance in other fields [4]. Within the language of molecular gauge theory [5], an effective non-zero magnetic flux passes through the symmetry point, i.e. the conical intersection (CI), of the model. In analog with the Aharonov-Bohm effect (ABE) effect, a wave packet evolving away from the CI, but still seem affected by the flux passing through it has been termed the molecular Aharonov-Bohm effect (MABE). Opposite to the ABE, Sjöqvist showed how the MABE can be interpreted as a local effect by assigning an electric force acting locally on the particle-motion [6]. We follow a different route and introduce a conjugate synthetic magnetic field, such that the corresponding Lorentz force is everywhere non-zero and give rise to a spin Hall effect [7]. Thereby, put in this dual representation, the MABE of linear JT models can be readily explained using arguments based on locality. It is important to point out that by *local* we have in mind a force acting locally on the phase space distribution.

Generalized gauge theory of the linear $E\times\varepsilon$ Jahn-Teller model. – For the linear $E\times\varepsilon$ JT model, the doubly degenerate vibrational mode with frequency ω will couple the two degenerate diabatic electronic states according to

$$\hat{H}_{E\times\varepsilon}=\omega\left(\frac{\hat{P}_x^2}{2}+\frac{\hat{P}_y^2}{2}+\frac{\hat{Q}_x^2}{2}+\frac{\hat{Q}_y^2}{2}\right)+k\left(\hat{Q}_x\hat{\sigma}_x+\hat{Q}_y\hat{\sigma}_y\right),\tag{1}$$

where $\hat{P}_{x,y}$ and $\hat{Q}_{x,y}$ are two sets of conjugate variables with $[\hat{Q}_{x,y},\hat{P}_{x,y}]=i$, and k is the JT coupling strength. The σ-operators are the standard Pauli matrices; $\hat{\sigma}_x=|1\rangle\langle2|+|2\rangle\langle1|$, $\hat{\sigma}_y=i\left(|1\rangle\langle2|-|2\rangle\langle1|\right)$, $\hat{\sigma}_z=|2\rangle\langle2|-|1\rangle\langle1|$, with $|1\rangle$ and $|2\rangle$ denoting the internal diabatic electronic states. Throughout this work we use atomic units.

In standard molecular gauge theory [5], the x- and y-components of the synthetic gauge potential are

$$\hat{A}_x^{(kl)}=-i\langle\psi_k|\partial_{Q_x}|\psi_l\rangle,\quad \hat{A}_y^{(kl)}=-i\langle\psi_k|\partial_{Q_y}|\psi_l\rangle\tag{2}$$

where the matrix-indices k and l are either $-$ or $+$, and the adiabatic states $|\psi_+\rangle=\left[\exp(-i\varphi/2)|1\rangle-\exp(i\varphi/2)|2\rangle\right]/\sqrt{2}$ and $|\psi_-\rangle=$

---

[*] Electronic address: jolarson@fysik.su.se

$[\exp(-i\varphi/2)|1\rangle + \exp(i\varphi/2)|2\rangle]/\sqrt{2}$, with the Q-dependent phase $\varphi = \arctan(Q_y/Q_x)$. The adiabatic states diagonalize the JT coupling part in Eq. (1). The overall phase ambiguity of the adiabatic states $|\psi_\pm\rangle$ represents the gauge freedom of the potential (2). The gauge independent magnetic field can be expressed in terms of the field tensor as $\hat{\mathbf{B}}_i = \frac{1}{2}\varepsilon_{ijk}\hat{\mathbf{F}}_{jk}$, where ε_{ijk} is the Levi-Cevita symbol and

$$\hat{\mathbf{F}}_{jk} = \partial_j\hat{\mathbf{A}}_k - \partial_k\hat{\mathbf{A}}_j - i[\hat{\mathbf{A}}_j, \hat{\mathbf{A}}_k]. \tag{3}$$

The last part of the field tensor derives from the matrix structure of the gauge potential, and whenever the two components $\hat{\mathbf{A}}_x$ and $\hat{\mathbf{A}}_y$ do not commute the system is said to be non-abelian. In terms of the $E \times \varepsilon$ JT model, this synthetic magnetic field vanishes everywhere except at the CI at $(Q_x, Q_y) = (0, 0)$, where it becomes singular; ergo also the Lorentz force must strictly disappear in the punctured Q_xQ_y-plane $\mathbb{R}\backslash(0,0)$. Moreover, since the adiabatic states $|\psi_\pm\rangle$ are independent on ω and k, it follows that also the magnetic field is independent on the system parameters.

Setting the JT coupling strength to zero, $k = 0$, results in a Hamiltonian of identical sets of two-dimensional harmonic oscillators. Let x, y, p_x, and p_y be the quantum expectation values of $\hat{Q}_x$, $\hat{Q}_y$, $\hat{P}_x$, and $\hat{P}_y$ respectively. For a Gaussian initial state displaced from the origin, the trajectories in phase space $(x(t), p_x(t))$ and $(y(t), p_y(t))$ will agree with the classical circular ones. To understand how the dynamics is affected by the JT coupling, let us rewrite the Hamiltonian as

$$\hat{H}_{E\times\varepsilon} = \omega\left[\frac{\left(\hat{Q}_x - \tilde{\mathbf{A}}_x\right)^2}{2} + \frac{\left(\hat{Q}_y - \tilde{\mathbf{A}}_y\right)^2}{2} + \frac{\hat{P}_x^2}{2} + \frac{\hat{P}_y^2}{2}\right] + \mathbf{\Phi}, \tag{4}$$

where $\tilde{\mathbf{A}}_{x,y} = -\frac{k}{\omega}\hat{\sigma}_{x,y}$ are the two components of the "conjugate" gauge vector potential, and $\mathbf{\Phi} = k^2/\omega$ the "conjugate" scalar potential. In this representation, the gauge potentials are constant but, due to their non-abelian character, give rise to a non-trivial conjugated magnetic field and a conjugate Lorentz force,

$$\tilde{\mathbf{B}}_z = -i[\tilde{\mathbf{A}}_x, \tilde{\mathbf{A}}_y] = 2\frac{k^2}{\omega^2}\hat{\sigma}_z, \quad \mathbf{F}_{cLor} = \frac{k^2}{2\omega^2}\hat{\sigma}_z(\hat{Q}_y, \hat{Q}_x). \tag{5}$$

The interpretation of Eq. (4) is a particle with two internal states moving in a harmonic potential influenced by a constant state-dependent magnetic field; if the particle is in the $|1\rangle$-state it sees a field pointing in the negative z-direction and the opposite holds for state $|2\rangle$. Unlike the synthetic magnetic field in the position representation, the conjugate magnetic field does depend on both ω and k. Consequently, it can not be seen as some sort of Fourier transform of the latter. Furthermore, put in a momentum representation, the JT coupling is nothing but a Rashba coupling [8] frequently appearing in condensed matter theories, such as the intrinsic anomalous and spin Hall effects [7].

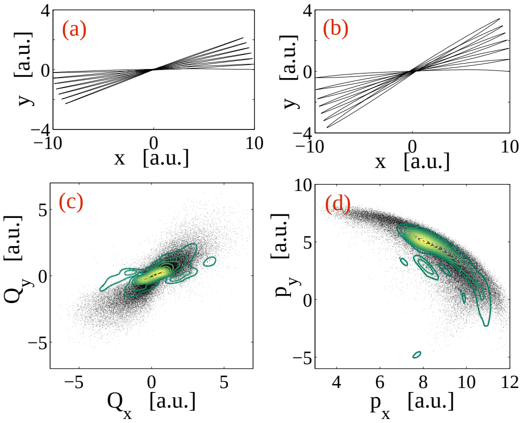

Figure 1: (Color online) In (a) the time evolution of the quantum expectation values $(x(t), y(t))$ are displayed, while (b) shows the corresponding semiclassical averaged trajectories obtained using the TWA approach. The final quantum density distributions in real and momentum space are depicted with contour-lines in (c) and (d), while the dots show the semi-classical distributions.

Numerical results of the linear $E \times \varepsilon$ JT model. – If we release a localized wave packet with initial expectation values $(p_x(0), p_y(0)) = (0, 0)$ and $(x(0), y(0)) = (x_0, 0)$, it appear reasonable to expect $y(t) = 0$ since the effective Lorentz force is strictly zero outside the CI and should not affect the dynamics as long as the wave packet is far from the CI. On the other hand, the conjugate effective Lorentz force of Eq. (5) is everywhere non-zero (in momentum space), and the propagation of the wave packet must be influenced accordingly. Since the Lorentz force is intrinsically acting in the transverse direction of motion, the wave packet has to build up a non-zero momentum $p_y(t)$ in the y-direction. This, in return, will cause a depletion from the $y(t) = 0$ trajectory, and our naive guess that $y(t) = 0$ must be wrong.

We numerically demonstrate this presumption by wave packet propagating, using the split-operator method [9] with an initial Gaussian state,

$$\psi(Q_x, Q_y, 0) = \left(\frac{1}{\pi\sigma^2}\right)^{1/4} \exp\left[-\frac{(Q_x - x_0)^2 + Q_y^2}{2\sigma^2}\right]|1\rangle, \tag{6}$$

with $x_0 = 10$ and the width $\sigma = 1$ corresponding to a coherent state given the frequency of the harmonic oscillators. The wave packet is propagated until $t = 15\,000$ a.u., and the parameter values, $k = 0.01$ a.u. and $\omega = 0.02$ a.u. The resulting trajectories of the expectation values $(x(t), y(t))$ are shown in Fig. 1 (a). Directly after the propagation has started, a positive $y(t)$ component builds up. As soon as the wave packet has crossed into negative Q_x, the effective force is reversed and $y(t)$ decreases again and at the first turning point, $x(t) \approx -10$ a.u., it has become negative $y(t) < 0$. When the evolution continues, a "bending" of the harmonic motion takes place in which vibrational excitations in the x-mode is swapped into excitation in the initially empty y-mode. This can be seen as a non-zero transverse current in the ϕ-direction, mimicking the intrinsic spin Hall effect [10]. The density $|\psi(Q_x, Q_y, t)|^2$ and its corresponding momentum density $|\phi(P_x, P_y, t)|^2$ of the final wave packet are displayed with solid contour lines in Fig. 1 (c) and (d). During the propagation the wave packet stays localized both in real and in momentum space, while for even longer times the wave packet, due to anharmonicities originating from the JT coupling, will spread out and cover more or less the entire accessible phase space [11].

The transverse current is a result from the JT coupling having the same structure as a Rashba coupling, known to give rise to Hall effects. In order to make the phenomenon more transparent we derive a set of semi-classical equations of motion, similar to those of Wong describing a classical color-charged particle in a non-abelian field [12],

$$\begin{array}{l}
\dot{x} = \omega p_x, \\
\dot{p}_x = -\omega x - k s_x, \\
\dot{y} = \omega p_y, \\
\dot{p}_y = -\omega y - k s_y, \\
\dot{s}_x = k y s_z, \\
\dot{s}_y = -k x s_z, \\
\dot{s}_z = k\left(x s_y - y s_x\right),
\end{array} \qquad (7)$$

where we recognize $s_\alpha = \langle\hat{\sigma}_\alpha\rangle$ with $\alpha = x,\, y,\, z$, and the dot indicates time derivative. Note that we denote the above semi-classical variables the same as the quantum expectation values, even though they are not equivalent in a strict sense. Indeed, the above set of equations does not take higher order quantum correlations into account, i.e. the equations are truncated and do not consider products like $(\dot{\widehat{xs_z}})$, $(\dot{\widehat{ys_x}})$ and so on. To extract some information about the conjugate Lorentz force, we take the derivative of $\dot{p}_x$ (or $\dot{p}_y$), $\ddot{p}_x = -\omega^2 p_x - k^2 y s_z$. This is the conjugate analog of Newton's second law. The first term on the right is the "acceleration" deriving from the harmonic motion, while the second is the state dependent part related to the conjugate Lorentz force being proportional to y.

The semi-classical approach is compared with the full quantum wave packet propagation using the truncated Wigner approximation (TWA), which has turned out to often reproduce the quantum dynamics surprisingly well [13]. Thus, we randomly sample initial values of positions and momentum according to the probability distributions $|\psi(Q_x, Q_y, 0)|^2$ and $|\phi(P_x, P_y, 0)|^2$ and propagate them using Eqs. (7). The expectation values displayed in Fig. 1 (b) are approximated with the averages over all trajectories. The final semi-classical distributions obtained from $N = 50\,000$ sampled trajectories are depicted in (c) and (d). It is found that this method somewhat overestimates the transverse motion, but still captures the quantitative features. This discrepancy is most likely due to large quantum fluctuations in the spin variables which is not captured in the above semi-classical analysis. As initial values for the spin isovector we used $S = (s_x, s_y, s_z) = (0, 0, 1)$ for all sampled trajectories, i.e. we have not taken initial quantum fluctuations into account for the internal two-level system [14].

In addition, for both the quantum and semi-classical approaches, we have numerically verified that the transverse force, i.e. the build-up of a transverse current, scales as $\sim k^2$ for short times as predicted according to Eq. (5). For longer times, due to the interplay between dynamics within the internal states, and dynamics arising from the effective Lorenz force and the harmonic oscillators, the evolution becomes rather complex, which is also known already for free Rashba coupled particles for which the problem is analytically solvable [15].

It is important to note that for the parameters k and ω, the ratio ω/k is larger than that obtained from *ab initio* calculations of the Li$_3$ molecule. As illustrated below when the dynamics on the two lower states of Li$_3$ is explored, the anharmonicity induced by the CI greatly destroys the harmonic motion and therefore also the regular structure of Fig. 1.

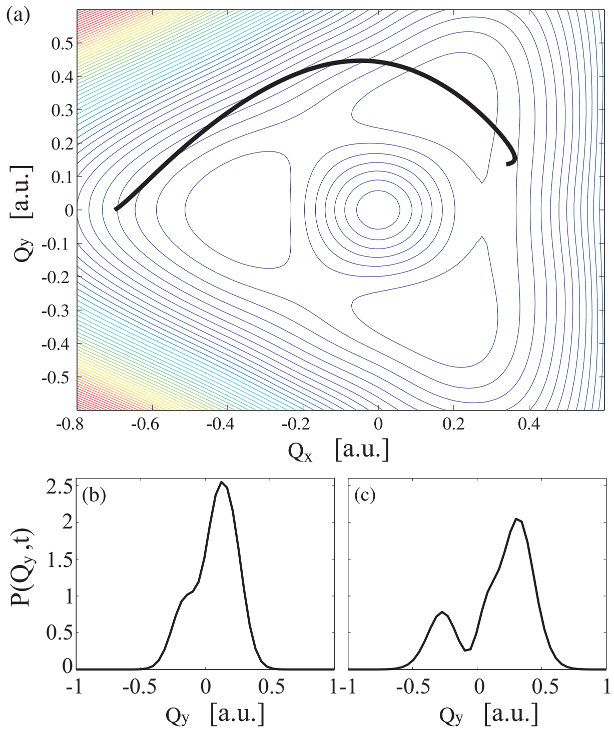

Figure 2: (Color online) The upper plot (a) shows the lower energy potential surface of the Li$_3$-trimer (contour lines) together with the quantum expectation values $x(t)$ and $y(t)$ (thick black line). The lower figures display the distribution $P(Q_y, t)$ at time instants, $t \approx 410$ a.u. (b) and $t \approx 820$ a.u. (c). The initial state is a Gaussian with $y(0) = p_x(0) = p_y(0) = 0$ a.u. and $x(0) = -0.7$ a.u., and width $\sigma = 1/2$ a.u. The final propagation time is approximately 4100 a.u. It is particularly clear how the system, as an appearance of the spin Hall effect, directly builds up a non-zero displacement in the Q_y-direction.

Effect in Li$_3$-trimer. – In the idealized case of the linearized $E\times\varepsilon$ JT model, the presence of a transverse force is clear from the momentum representation of the problem. Once higher order terms are taken into account, i.e. the coupling and the potential are no longer linear and quadratic respectively, introducing a conjugate gauge potential is non-trivial. Nevertheless, we may expect that the dynamics should still be greatly influenced by effects deriving from linear order terms. Thus, as for the above example, the augmentation of a transverse current is taken as a smoking gun for a spin Hall effect which in return can be ascribed some synthetic Lorentz force.

As a demonstrating example we consider the Li$_3$ molecule which possesses a CI between its two lowest electronic states [16]. More precisely, the Li$_3$ molecule possesses three vibrational normal modes corresponding to bending, asymmetric stretching, and symmetric stretching modes, which are all taken into account in our analysis. The adiabatic potential energy surfaces are computed with the MOLPRO program package [17] using the Multi-Reference Configuration Interaction (MRCI) method with molecular orbitals obtained from the state-averaged Multi-Configuration Self Consistent Field (MCSCF) calculations with an active space consisting of three electrons distributed among fifteen orbitals (all molecular orbitals composed of $2s$ and $2p$ atomic orbitals). The MRCI calculations are performed using the same reference space as for the MCSCF calculations. Excitations out of the core orbitals as well as single and double external excitations are all included. The calculations are carried out using the aug-cc-PVTC basis set [18]. By least square fitting of the computed two lowest adiabatic potential energy surfaces to the eigenvalues of the potential part of the JT Hamiltonian, the corresponding JT parameters can be obtained [19]. Here, in addition to the linear terms, the fitted Hamiltonian also contains quadratic and cubic anharmonic terms. The obtained JT parameters are used to determine the adiabatic to diabatic transformation matrix. Then the *ab initio* computed adiabatic potential energy surfaces are transformed into the diabatic potentials and couplings used for the wave packet propagation. A reliable description of the system Hamiltonian is then obtained also far from the conical intersection, where the Jahn-Teller Hamiltonian is no longer a good approximation [19]. The details of the numerical procedures for the Li3-calculations, together with corresponding results of the potentials, will be published elsewhere [20].

The full three-dimensional wave packet propagation is carried out using the Multi-Configurational Time-Dependent Hartree method [21]. The initial state is a real valued Gaussian with width $\sigma = 1/2$ located at the lower adiabatic potential surface at $(Q_x, Q_y, Q_s) = (-0.7, 0, 3.2)$. For this choice, the initial state is, to a good approximation, not in contact with the synthetic flux through the CI. The value $Q_s = 3.2$ corresponds to a global minima in this coordinate, and the dynamics should predominantly appear in the Q_x and Q_y coordinates corresponding to bending and asymmetric stretching. The lower potential surface is symmetric with respect to $Q_y = 0$ (see Fig. 2), and, as for the linear $E\times\varepsilon$ JT model, this implies that a non-zero $y(t)$ signals a spin Hall effect. The numerical results are presented in Fig. 2, showing the trajectory $(x(t), y(t)) = (\langle\hat{Q}_x\rangle, \langle\hat{Q}_y\rangle)$ with a thick line in (a), and two snap-shots of the projected distribution $P(Q_y, t) = \int dQ_x|\psi(Q_x, Q_y, t)|^2$ in (b) and (c). The final propagation time in (a) is 4100 a.u. The instantaneous build-up of a transverse force/current is clearly demonstrated in the figure, and note that the sign of this force is in accordance with our previously introduced conjugated Lorenz force. This is also demonstrated in the asymmetry of the projected distributions already seen at very short times. Due to large anharmonicities, the wave packet rapidly spreads and the effect is therefore only visible for short times.

Conclusion. – Using knowledge of the dual model of the $E\times\epsilon$ JT Hamiltonian, we demonstrated how the corresponding MABE can be attributed only to local forces. In the conjugate picture, the inherent gauge potentials are non-abelian and constitute an everywhere non-zero Lorentz force which causes a wave packet far from the CI to deflect from its expected classical trajectory. In condensed matter theories, the same mechanism is essential for; the spin Hall effect, topological insulators, high-T superconductors, Dirac and majorana fermions, just to mention a few examples. In this respect, the present work bridge two of the main fields of physics, molecular and condensed matter, and our results suggest that known effects in one field can be translated into the other.

Our dual picture analysis is exact in the linear case, but is not apparent when non-harmonicity and the extra degree-of-freedom are taken into account. Using a full quantum calculation, taking all degrees-of-freedom into account as well as all higher orders in the JT model, we also presented evidences how the intrinsic asymmetry of the Li$_3$ molecule dynamics can be assigned a spin Hall effect.

Acknowledgments

We thank Hans Hansson and Erik Sjöqvist for valuable discussions. JL acknowledges support from the Swedish research council (VR), Deutscher Akademischer Austausch Dienst (DAAD), and Kungl. Vetenskapsakademien (KVA). ÅL acknowledges support from the Swedish research council (VR).

[1] Y. Aharonov and D. Bohm, Phys. Rev. **115**, 485 (1959).

[2] I. B. Bersuker, *The Jahn-Teller Effect*, (Cambridge Uni-

versity Press, Cambridge, 2006).

[3] H. C. Longuet-Higgins *et al.*, Proc. R. Soc. London Ser. A **244**, 1 (1958).

[4] J. Larson and S. Levin, Phys. Rev. Lett. **103**, 013602 (2009); J. Larson and E. Sjöqvist, Phys. Rev. A **79**, 043627 (2009); T. Dereli *et al.*, arXiv:1109.1199.

[5] D. Bohm *et al.*, *Geometric Phase in Quantum Mechanics*, (Springer-Verlag).

[6] E. Sjq̈vist, Phys. Rev. Lett. **89**, 210401 (2002).

[7] J. Sinova *et al.*, Phys. Rev. Lett. **92**, 126603 (2004); N. Nagaosa *et al.*, Rev. Mod. Phys. **82**, 1539 (2010).

[8] Y. A. Bychov and E. I. Rashba, J. Phys. C **17**, 6039 (1984).

[9] M. D. Fleit *et al.*, J. Comput. Phys. **47**, 412 (1982).

[10] J. Larson, Phys. Rev. A **81**, 051803(R) (2010).

[11] By "accessible" we mean the surface of phase space bounded to the energies of the initial state.

[12] S. K. Wong, Nuovo Cimento **65** A, 689 (1979).

[13] A. Polkovnikov, Annals of Phys. **325**, 1790 (2010).

[14] One could include spin fluctuations in the analysis by representing it in terms of spin coherent states, but since we are only interested in the qualitative behavior we do not find this necessary, and furthermore.

[15] J. Larson *et al.*, Phys. Rev. A **82**, 043620 (2010).

[16] T. C. Thompson, D. G. Truhlar, and C. A. Maed, J. Chem. Phys., **82**, 2392-2407 (1985); T. C. Thompson, G. Izmirlian, S. J. Lemon, D. G. Truhlar, and C. A. Maed, J. Chem. Phys., **82**, 5597-5603 (1985).

[17] MOLPRO, version 2010.1, a package of *ab initio* programs. H.-J. Werner, P. J. Knowles, G. Knizia, F. R. Manby, M. Schütz, and others, See http://www.molpro.net.

[18] T.H. Dunning Jr., J. Chem. Phys. 90, 1007 (1989).

[19] J. Schön and H. Köppel, J. Chem. Phys., **108**, 1503 (1998).

[20] E. N. Ghassemi *et al.*, To be published.

[21] The MCTDH Package, Version 8.4 (2007). G. A. Worth and M. H. Beck and A. Jäckle and H.-D. Meyer, See http://mctdh.uni-hd.de, University of Heidelberg, Germany.